

# Leptophilic Interactions in Nuclear Energy Density Functional Theory

S. O. Kara<sup>1</sup>

<sup>1</sup>*Niğde Ömer Halisdemir University, Bor Vocational School, Niğde, Türkiye*

(Dated: December 15, 2025)

We develop a unified framework that embeds a light leptophilic vector boson  $Z_\ell$  into nuclear energy-density functional theory. Starting from the underlying gauge interaction and integrating out the mediator in the static limit, we derive a leptophilic current-current term that is incorporated self-consistently into relativistic mean-field equations. The resulting leptophilic energy-density functional (L-EDF) produces correlated modifications of proton and lepton chemical potentials, leading to percent-level changes in the proton fraction, symmetry energy, and equation of state of  $\beta$ -equilibrated matter. For finite nuclei, the interaction induces shifts of  $10^{-3}$ – $10^{-2}$  fm in neutron-skin thicknesses, comparable to current experimental sensitivities. The framework thus links nuclear structure and dense matter to new physics in the leptonic sector, providing a realistic and experimentally testable deformation of conventional energy-density functionals.

## I. INTRODUCTION

The structure of atomic nuclei and the properties of cold dense matter are governed by the interplay of hadronic interactions, many-body correlations, and the symmetries of the Standard Model (SM). Energy-density functional (EDF) theory provides a powerful and systematically improvable framework for describing these systems across the nuclear chart [1, 2]. Modern covariant (relativistic) EDFs, based on Walecka-type Lagrangians and their density-dependent extensions, successfully reproduce binding energies, charge radii, neutron-skin thicknesses, and the nuclear equation of state (EoS) [3–6].

At the same time, there has been growing interest in physics beyond the SM featuring new interactions that couple preferentially to leptons. Such leptophilic sectors arise naturally in anomaly-free  $U(1)'$  extensions [7], in models with light hidden vectors [8, 9], and in neutrino-portal or sterile-neutrino scenarios [10]. While these interactions are often studied in particle-physics or astrophysical contexts, their potential impact on nuclear systems remains comparatively unexplored.

Leptophilic interactions directly modify lepton densities and chemical potentials, and therefore affect the conditions of  $\beta$  equilibrium in dense matter. As a consequence, they can induce correlated shifts in proton fractions, isovector properties, and bulk thermodynamic observables that enter the nuclear EoS. In finite nuclei, such effects propagate through the proton mean field and can modify neutron-skin thicknesses and isovector density profiles. These observables are known to be sensitive probes of the symmetry energy and its density dependence [11, 12].

In this work we develop a unified framework that embeds a light leptophilic vector boson,  $Z_\ell$ , into relativistic nuclear EDF theory. By integrating out the mediator in the static limit, we obtain an effective current-current interaction that couples the proton and lepton sectors and can be implemented self-consistently at the mean-field level. The resulting leptophilic EDF (L-EDF) constitutes

a controlled deformation of standard RMF functionals.

We apply the L-EDF framework to both uniform nuclear matter in  $\beta$  equilibrium and to selected finite nuclei. We demonstrate that leptophilic interactions induce percent-level modifications in the proton fraction, symmetry energy, and EoS of dense matter, as well as measurable shifts in neutron-skin thicknesses. These effects are comparable in magnitude to current experimental sensitivities and to the intrinsic spread among modern EDF parametrizations, establishing nuclear structure and dense matter as promising laboratories for probing new physics in the leptonic sector.

## II. FORMALISM

### A. Leptophilic gauge sector

We introduce a new Abelian gauge interaction  $U(1)'_\ell$  under which the charged leptons (and, optionally, neutrinos) carry vector-like charges, following generic anomaly-free constructions discussed in Refs. [7, 13]. At the renormalizable level, the leptophilic mediator  $Z_\ell$  is described by the Lagrangian

$$\mathcal{L}_\ell = -\frac{1}{4} Z_{\ell\mu\nu} Z_\ell^{\mu\nu} + \frac{1}{2} m_{Z_\ell}^2 Z_{\ell\mu} Z_\ell^\mu + g_\ell Z_{\ell\mu} J_\ell^\mu, \quad (1)$$

where  $Z_{\ell\mu\nu} = \partial_\mu Z_{\ell\nu} - \partial_\nu Z_{\ell\mu}$  denotes the field-strength tensor and  $m_{Z_\ell}$  is the mediator mass. The leptonic current is given by

$$J_\ell^\mu = \sum_{f=e,\mu,\tau,\nu_e,\nu_\mu,\nu_\tau} \bar{f} \gamma^\mu f, \quad (2)$$

and couples universally to the leptophilic gauge boson with strength  $g_\ell$ .

A small but phenomenologically relevant coupling to hadrons is induced via kinetic mixing between the hypercharge gauge field and the leptophilic vector  $Z_\ell$  [13],

$$\mathcal{L}_{\text{mix}} = -\frac{\varepsilon}{2} B_{\mu\nu} Z_\ell^{\mu\nu}, \quad (3)$$

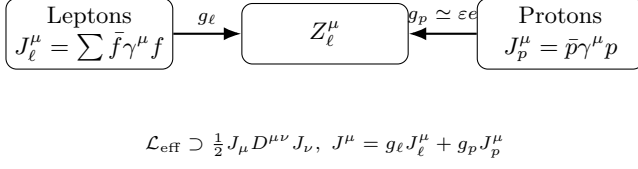


FIG. 1. Schematic illustration of the leptophilic mediator  $Z_\ell$  coupling to lepton and proton currents. The effective interaction relevant for nuclear systems is governed by the combined current  $J^\mu = g_\ell J_\ell^\mu + g_p J_p^\mu$ .

where  $\varepsilon$  denotes the kinetic-mixing parameter. After electroweak symmetry breaking, this interaction generates an effective coupling of  $Z_\ell$  to the proton current,

$$\mathcal{L}_p^{\text{eff}} \simeq g_p Z_\ell \bar{p} \gamma^\mu p, \quad g_p \simeq \varepsilon e, \quad (4)$$

up to model-dependent factors associated with electroweak mixing. In the following analysis,  $g_p$  is treated as an effective parameter that encapsulates all hadronic sources of  $Z$ - $Z_\ell$  mixing, allowing for a model-independent implementation within the EDF framework.

A schematic overview of the resulting leptophilic couplings is shown in Fig. 1.

## B. Integrating out the mediator: current-current structure

In nuclear systems the characteristic momenta satisfy  $k_F \ll m_{Z_\ell}$  for mediator masses above the MeV scale, allowing the heavy vector field to be integrated out in the static limit. Starting from the interaction

$$\mathcal{L}_{\text{int}} = Z_\ell \mu (g_\ell J_\ell^\mu + g_p J_p^\mu), \quad J_p^\mu \equiv \bar{p} \gamma^\mu p, \quad (5)$$

one obtains the classical equation of motion

$$(-\nabla^2 + m_{Z_\ell}^2) Z_\ell^0(\mathbf{r}) = J^0(\mathbf{r}), \quad (6)$$

with the combined source  $J^0 = g_\ell n_\ell + g_p n_p$ .

The solution of Eq. (6) involves the Yukawa Green's function,

$$Z_\ell^0(\mathbf{r}) = \int d^3 r' G_Y(\mathbf{r} - \mathbf{r}') J^0(\mathbf{r}'), \quad (7)$$

$$G_Y(\mathbf{r}) = \frac{1}{4\pi} \frac{e^{-m_{Z_\ell} |\mathbf{r}|}}{|\mathbf{r}|}. \quad (8)$$

Substituting this solution back into the Lagrangian yields the nonlocal current-current contribution to the energy density functional,

$$\mathcal{E}_{Z_\ell} = \frac{1}{2} \int d^3 r d^3 r' G_Y(\mathbf{r} - \mathbf{r}') \mathcal{J}(\mathbf{r}) \mathcal{J}(\mathbf{r}'), \quad (9)$$

where the effective source is given by

$$\mathcal{J}(\mathbf{r}) = g_\ell n_\ell(\mathbf{r}) + g_p n_p(\mathbf{r}). \quad (10)$$

## C. Local limit and Kohn-Sham potentials

In the limit  $m_{Z_\ell} \gg k_F$  the interaction becomes effectively local,

$$G_Y(\mathbf{r} - \mathbf{r}') \simeq \frac{1}{m_{Z_\ell}^2} \delta^{(3)}(\mathbf{r} - \mathbf{r}'), \quad (11)$$

leading to the local energy density

$$\mathcal{E}_{Z_\ell}^{(\text{loc})} = \frac{1}{2m_{Z_\ell}^2} [g_\ell n_\ell(\mathbf{r}) + g_p n_p(\mathbf{r})]^2. \quad (12)$$

The corresponding Kohn-Sham mean fields are obtained by functional differentiation with respect to the densities,

$$V_p^{Z_\ell}(\mathbf{r}) = \frac{\delta \mathcal{E}_{Z_\ell}}{\delta n_p(\mathbf{r})}, \quad V_\ell^{Z_\ell}(\mathbf{r}) = \frac{\delta \mathcal{E}_{Z_\ell}}{\delta n_\ell(\mathbf{r})}. \quad (13)$$

In the local limit these reduce to

$$V_p^{Z_\ell}(\mathbf{r}) = \frac{g_p}{m_{Z_\ell}^2} [g_\ell n_\ell(\mathbf{r}) + g_p n_p(\mathbf{r})], \quad (14)$$

$$V_\ell^{Z_\ell}(\mathbf{r}) = \frac{g_\ell}{m_{Z_\ell}^2} [g_\ell n_\ell(\mathbf{r}) + g_p n_p(\mathbf{r})]. \quad (15)$$

## D. RMF embedding of the L-EDF

To obtain quantitative predictions, we embed the leptophilic functional into a standard relativistic mean-field (RMF) framework with  $\sigma$ - $\omega$ - $\rho$  meson fields [4, 5]. In static, spin-saturated nuclear matter the nucleonic Lagrangian reads

$$\mathcal{L}_{\text{had}} = \bar{\psi}_N \left[ \gamma_\mu (i\partial^\mu - g_\omega \omega_0 \delta_0^\mu - g_\rho \tau_3 \rho_{03} \delta_0^\mu) - (m_N - g_\sigma \sigma_0) \right] \psi_N + \mathcal{L}_{\sigma, \omega, \rho}, \quad (16)$$

with mean fields  $\sigma_0$ ,  $\omega_0$ , and  $\rho_{03}$ .

The corresponding field equations are

$$m_\sigma^2 \sigma_0 = g_\sigma (n_s^n + n_s^p), \quad (17)$$

$$m_\omega^2 \omega_0 = g_\omega (n_n + n_p), \quad (18)$$

$$m_\rho^2 \rho_{03} = g_\rho (n_p - n_n), \quad (19)$$

$$m_{Z_\ell}^2 Z_\ell^0 = g_\ell n_\ell + g_p n_p. \quad (20)$$

The Dirac effective mass is defined as  $m^* = m_N - g_\sigma \sigma_0$ . The neutron and proton chemical potentials become

$$\mu_n = \sqrt{k_{F,n}^2 + m^{*2}} + g_\omega \omega_0 - g_\rho \rho_{03}, \quad (21)$$

$$\mu_p = \sqrt{k_{F,p}^2 + m^{*2}} + g_\omega \omega_0 + g_\rho \rho_{03} + g_p Z_\ell^0. \quad (22)$$

Leptons are treated as relativistic Fermi gases subject to the same vector shift,

$$\mu_e = \sqrt{k_{F,e}^2 + m_e^2} + g_\ell Z_\ell^0, \quad (23)$$

$$\mu_\mu = \sqrt{k_{F,\mu}^2 + m_\mu^2} + g_\ell Z_\ell^0. \quad (24)$$

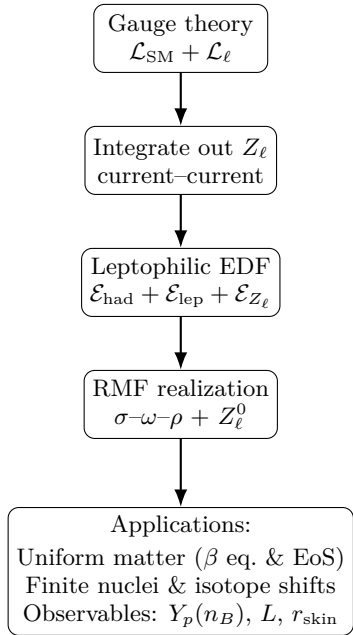


FIG. 2. From the leptophilic gauge sector to the density functional, its RMF embedding, and the main applications considered in this work.

This coupled set of mean-field equations defines the relativistic realization of the L-EDF. The conceptual flow from the leptophilic gauge sector to the EDF and its RMF embedding is summarized in Fig. 2.

### E. Beta equilibrium and charge neutrality

Cold catalyzed matter in neutron-star and dense-matter environments satisfies the conditions of beta equilibrium,

$$\mu_n = \mu_p + \mu_e, \quad (25)$$

$$\mu_e = \mu_\mu \quad (\mu_e > m_\mu), \quad (26)$$

together with the requirement of electric charge neutrality,

$$n_p = n_e + n_\mu. \quad (27)$$

Equations (25)–(27), combined with the self-consistent mean-field equations introduced above, uniquely determine the proton fraction  $Y_p = n_p/n_B$  and the lepton densities for a given baryon density  $n_B$ .

Within the L-EDF framework, the leptophilic mean field  $Z_\ell^0$  provides a direct dynamical link between the proton and lepton sectors. As a result, modifications of the lepton chemical potentials feed back into the hadronic equilibrium conditions, leading to correlated shifts in the proton fraction, symmetry energy, and related observables in both uniform matter and finite nuclei.

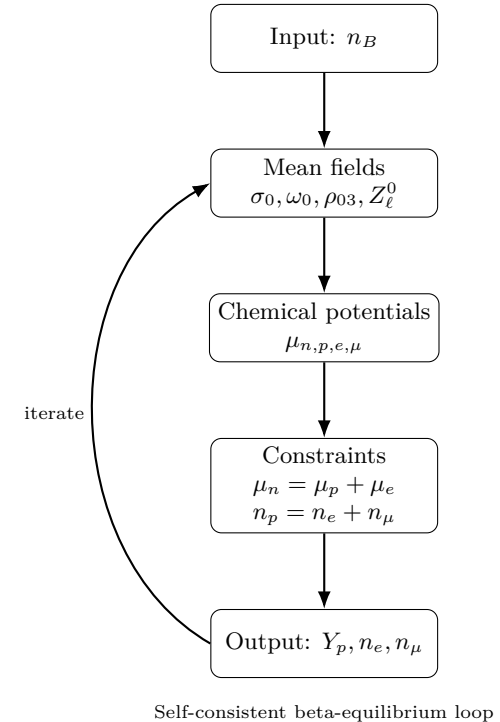


FIG. 3. Self-consistent determination of the proton fraction and lepton densities in cold, beta-equilibrated nuclear matter within the leptophilic EDF framework. For a fixed baryon density  $n_B$ , the mean fields  $\sigma_0$ ,  $\omega_0$ ,  $\rho_{03}$ , and the leptophilic vector field  $Z_\ell^0$  are iteratively updated together with the chemical potentials until the beta-equilibrium and charge-neutrality conditions are simultaneously satisfied.

## III. RESULTS AND DISCUSSION

In this section we quantify the impact of the leptophilic energy-density functional (L-EDF) introduced above. We consider three complementary settings: (i) uniform nuclear matter in beta equilibrium, (ii) symmetry-energy systematics and neutron-skin thicknesses of finite nuclei, and (iii) low-density limits relevant for atomic isotope shifts. In all three cases the leptophilic interaction generates correlated modifications of the proton and lepton sectors that cannot be captured by conventional hadronic functionals based on standard relativistic mean-field (RMF) approaches [2, 3, 5, 14].

### A. Uniform matter and beta equilibrium

We solve the coupled mean-field and beta-equilibrium conditions, Eqs. (25)–(27), across a representative range of baryon densities,  $n_B = 0.5 n_0$ – $3 n_0$ , where  $n_0 \simeq 0.16 \text{ fm}^{-3}$  denotes the empirical saturation density. The numerical implementation follows a fully self-consistent iteration cycle in which the mean fields, particle fractions, and chemical potentials are updated until convergence, as summarized in Fig. 3. Such iterative schemes are stan-

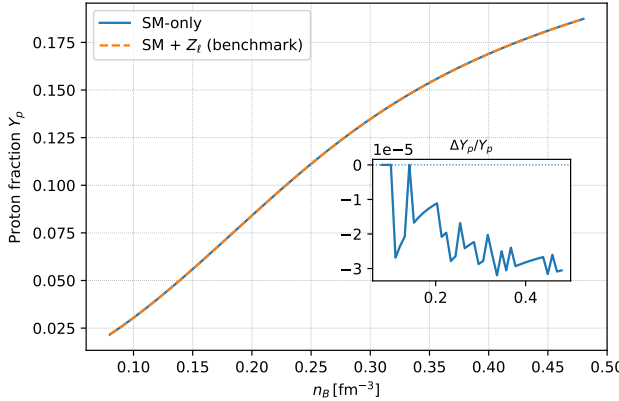


FIG. 4. Proton fraction  $Y_p$  in beta-equilibrated matter. Solid: Standard-Model-only baseline. Dashed: leptophilic benchmark with  $m_{Z_\ell} = 10$  MeV,  $g_\ell = 10^{-3}$ ,  $g_p = 10^{-4}$ . The enhancement reflects the effective repulsion generated by the shared leptophilic mean field.

dard in dense-matter and RMF calculations [15–17].

Unless stated otherwise, we use the well-established DD-ME2 and NL3 parameter sets for the hadronic sector [5, 14]. The leptophilic sector is explored over the representative range  $m_{Z_\ell} = 5–100$  MeV,  $g_\ell = 10^{-4}–10^{-2}$ ,  $g_p = \varepsilon e$ ,  $\varepsilon = 10^{-6}–10^{-3}$ , consistent with laboratory, astrophysical, and cosmological bounds on light vectors [18–21].

Figure 4 shows the resulting proton fraction. Two robust trends appear:

(i) The leptophilic mean field  $Z_\ell^0$  generates an effective repulsion between the proton and lepton sectors, lowering the electron chemical potential and increasing the equilibrium proton fraction relative to standard RMF predictions [11, 12]. The shift approximately scales with  $g_\ell g_p/m_{Z_\ell}^2$ .

(ii) At  $n_B \gtrsim 2n_0$ , muon onset provides an additional leptonic source, enhancing the Hartree term  $g_\ell n_\ell + g_p n_p$  and amplifying deviations from the SM-only baseline [15].

Even within existing bounds, the net modification of  $Y_p$  reaches the few-percent level, comparable to the spread among modern EDF predictions [22].

## B. Equation of state and symmetry-energy slope

The leptophilic interaction modifies the nuclear equation of state (EoS) through two channels: (i) changes in the proton fraction alter the isovector composition of matter, and (ii) the vector term  $g_p Z_\ell^0$  contributes directly to the proton chemical potential. Consequently, the pressure,  $P(n_B) = n_B^2 \partial(\mathcal{E}/n_B)/\partial n_B$ , exhibits shifts at the level of  $\Delta P/P \sim 1–5\%$ , comparable to differences among modern RMF parametrizations [11, 23].

Figure 5 summarizes these modifications. Intermediate densities show mild softening, while higher densities ex-

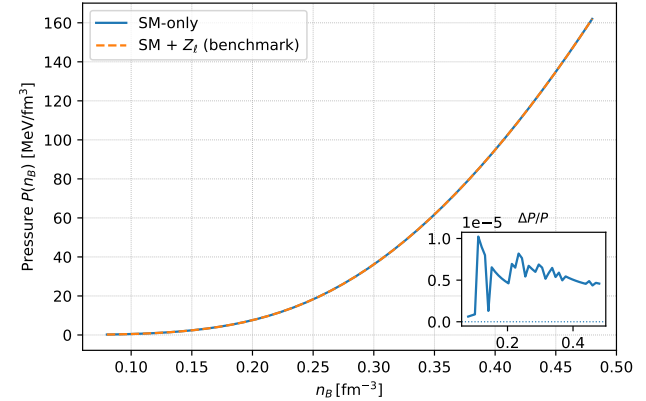


FIG. 5. Pressure of beta-equilibrated matter. Solid: Standard-Model-only. Dashed: leptophilic benchmark ( $m_{Z_\ell} = 10$  MeV,  $g_\ell = 10^{-3}$ ,  $g_p = 10^{-4}$ ). Leptophilic contributions induce  $\mathcal{O}(1\%–5\%)$  variations, similar to the spread among modern RMF parametrizations.

hibit slight stiffening—both driven by the correlated evolution of proton and lepton contributions to the shared mean field. These trends remain within empirical bounds on the symmetry energy and its slope [6, 24].

The symmetry energy  $S(n_B)$  and its slope  $L = 3n_0 (\partial S/\partial n)|_{n_0}$  are especially sensitive to proton-fraction modifications [11, 12]. Benchmark couplings yield  $\Delta L \simeq 2–8$  MeV, consistent with PREX-II and CREX uncertainties [25, 26].

Figure 6 displays the symmetry-energy density dependence. The leptophilic benchmark induces a characteristic upward shift proportional to  $g_\ell g_p/m_{Z_\ell}^2$ , feeding directly into  $L$ .

## C. Finite nuclei: neutron-skin thickness and radii

In finite nuclei the leptophilic vector contributes to the proton mean field  $V_p^{Z_\ell}$ , generating small correlated shifts in single-particle energies and in the isovector density profile. RMF calculations for  $^{48}\text{Ca}$ ,  $^{90}\text{Zr}$ , and  $^{208}\text{Pb}$  indicate that benchmark couplings produce neutron-skin modifications of  $\Delta r_{\text{skin}} \simeq 0.005–0.02$  fm, compatible with PREX/CREX sensitivities and typical responses to weak isovector perturbations [25–28].

## D. Summary of nuclear-matter and finite-nucleus effects

Across all observables—proton fraction, EoS, symmetry energy, and neutron-skin thickness—the leptophilic mean field introduces coherent, density-dependent modifications governed by  $g_\ell g_p/m_{Z_\ell}^2$ . Within phenomenologically allowed parameter ranges, these effects amount to  $\mathcal{O}(1\%–5\%)$  variations in uniform matter and  $\Delta r_{\text{skin}} \sim$

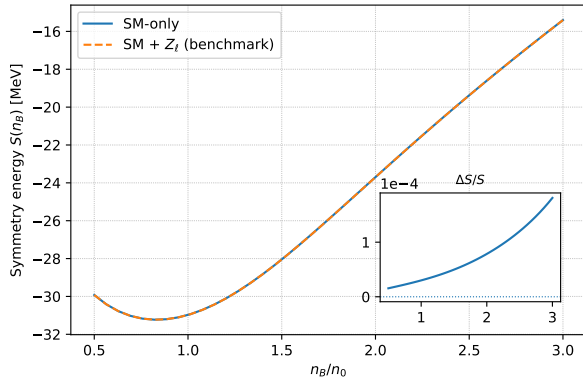


FIG. 6. Symmetry-energy function  $S(n_B)$  obtained in the L-EDF framework. The leptophilic mean field induces an upward shift scaling with  $g_\ell g_p/m_{Z_\ell}^2$ , which propagates into the slope parameter  $L$  at saturation.

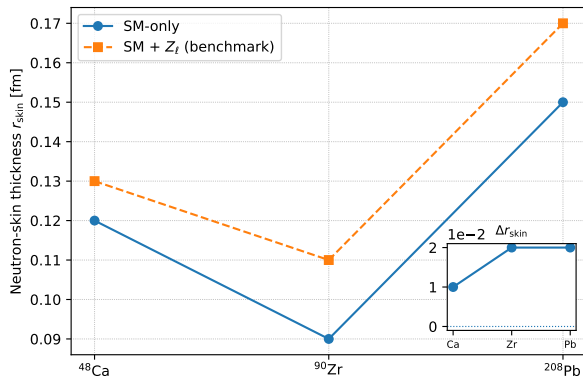


FIG. 7. Neutron-skin thickness  $r_{\text{skin}}$  for selected nuclei. Solid: Standard-Model-only baseline. Dashed: leptophilic benchmark ( $m_{Z_\ell} = 10$  MeV,  $g_\ell = 10^{-3}$ ,  $g_p = 10^{-4}$ ). Predicted shifts  $\Delta r_{\text{skin}} \sim 0.005\text{--}0.02$  fm match PREX/CREX sensitivity ranges.

0.005–0.02 fm in finite nuclei. Such magnitudes are

comparable to the spread among modern EDFs and fall within current experimental reach, demonstrating that nuclear-structure observables constitute a sensitive probe of leptophilic interactions.

#### IV. CONCLUSIONS

We have constructed a unified theoretical framework in which a light leptophilic vector boson  $Z_\ell$  is consistently embedded into nuclear energy–density functional theory. Starting from the underlying gauge interaction, integrating out the mediator in the static limit, and incorporating the resulting current–current interaction into relativistic mean-field dynamics, we obtained a leptophilic extension of standard hadronic EDFs (L-EDF). This provides a self-consistent and systematically improvable approach for exposing nuclear structure and dense-matter observables to new physics in the leptonic sector.

The L-EDF modifies both proton and lepton chemical potentials through the shared mean field  $Z_\ell^0$ , leading to correlated shifts in the proton fraction, symmetry energy, and equation of state of  $\beta$ -equilibrated matter. For representative benchmark points compatible with current laboratory and astrophysical constraints, these effects reach the percent level in bulk matter and the  $10^{-3}\text{--}10^{-2}$  fm level in neutron-skin thicknesses of finite nuclei. The magnitude of these shifts is comparable to the spread among modern EDF parametrizations, indicating that leptophilic interactions constitute a realistic and experimentally testable deformation of nuclear phenomenology rather than a negligible perturbation.

Taken together, our results demonstrate that light leptophilic vectors leave correlated and experimentally accessible imprints in both uniform matter and finite nuclei. The framework introduced here can be extended to global refits of L-EDF parameters, applications to realistic neutron-star matter, and combined analyses of nuclear and astrophysical observables, providing a new avenue for probing leptophilic interactions through nuclear structure.

- 
- [1] M. Bender, P.-H. Heenen, and P.-G. Reinhard, *Rev. Mod. Phys.* **75**, 121 (2003).  
[2] P. Ring, *Prog. Part. Nucl. Phys.* **37**, 193 (1996).  
[3] P.-G. Reinhard, *Rep. Prog. Phys.* **52**, 439 (1989).  
[4] B. D. Serot and J. D. Walecka, *Adv. Nucl. Phys.* **16**, 1 (1986).  
[5] G. A. Lalazissis, T. Nikšić, D. Vretenar, and P. Ring, *Phys. Rev. C* **71**, 024312 (2005).  
[6] L.-W. Chen, *Sci. China Phys. Mech. Astron.* **54**, 124 (2011).  
[7] J. Heeck, *Phys. Lett. B* **739**, 256 (2014).  
[8] B. Batell, M. Pospelov, and A. Ritz, *Phys. Rev. D* **80**, 095024 (2009).  
[9] M. Pospelov, *Phys. Rev. D* **80**, 095002 (2009).  
[10] P. Ballett *et al.*, *JHEP* **09**, 152 (2020).  
[11] M. B. Tsang *et al.*, *Phys. Rev. C* **86**, 015803 (2012).  
[12] J. M. Lattimer, *Annu. Rev. Nucl. Part. Sci.* **62**, 485 (2012).  
[13] B. Holdom, *Phys. Lett. B* **166**, 196 (1986).  
[14] G. A. Lalazissis *et al.*, *Phys. Rev. C* **82**, 045501 (2010).  
[15] M. Prakash *et al.*, *Phys. Rep.* **280**, 1 (1997).  
[16] A. Burrows and J. M. Lattimer, *Astrophys. J.* **307**, 178 (1986).  
[17] S. L. Shapiro and S. A. Teukolsky, *Black Holes, White Dwarfs, and Neutron Stars*, Wiley (1983).  
[18] E. Hardy and R. Lasenby, *JHEP* **02**, 033 (2017).  
[19] E. Rrapaj and S. Reddy, *Phys. Rev. C* **94**, 045805 (2016).  
[20] J. H. Chang *et al.*, *JHEP* **09**, 051 (2018).

- [21] S. Knapen *et al.*, *Phys. Rev. Lett.* **118**, 171801 (2017).
- [22] C. J. Horowitz and J. Piekarewicz, *Phys. Rev. Lett.* **86**, 5647 (2001).
- [23] B. A. Brown, *Phys. Rev. Lett.* **111**, 232502 (2013).
- [24] X. Roca-Maza *et al.*, *Phys. Rev. C* **92**, 064304 (2015).
- [25] D. Adhikari *et al.*, *Phys. Rev. Lett.* **126**, 172502 (2021).
- [26] D. Adhikari *et al.*, *Phys. Rev. Lett.* **129**, 042501 (2022).
- [27] F. J. Fattoyev and J. Piekarewicz, *Phys. Rev. C* **86**, 015802 (2012).
- [28] P.-G. Reinhard *et al.*, *Phys. Rev. C* **101**, 021301 (2020).